IEEE Access
Multidisciplinary | Rapid Review | Open Access Journal

Received January 14, 2019, accepted January 26, 2019, date of publication February 11, 2019, date of current version March 5, 2019.

Digital Object Identifier 10.1109/ACCESS.2019.2898513

Design Analysis of Integrated Passive Device-Based Balun Devices With High Selectivity for Mobile Application

ALOK KUMAR[1], FAN-YI MENG[1], (Senior Member, IEEE), CONG WANG[1], (Senior Member, IEEE), KISHOR KUMAR ADHIKARI[1], TIAN QIANG[1], (Member, IEEE), QUN WU[1], (Senior Member, IEEE), AND YONGLE WU[2], (Senior Member, IEEE)

[1]School of Electronics and Information Engineering, Harbin Institute of Technology, Harbin 150001, China
[2]School of Electronic Engineering, Beijing University of Posts and Telecommunications, Beijing 100876, China

Corresponding authors: Cong Wang (kevinwang@hit.edu.cn) and Yongle Wu (wuyongle138@gmail.com)

This work was supported in part by the Natural Science Foundation of China under Grant 61801146, in part by the China Postdoctoral Science Foundation under Grant 2017M611367 and Grant 2018M641813, in part by the Heilongjiang Postdoctoral Fund under Grant LBH-Z17056, and in part by the Fundamental Research Fund for the Central Universities.

ABSTRACT This paper presents highly selective, low-loss, and miniaturized balun devices fabricated using the integrated passive device (IPD) technique for the GSM band (900/1800 MHz) and the WiFi band (2400 MHz) in mobile applications. Balun devices were fabricated on a gallium arsenide (GaAs) substrate using the IPD fabrication process to reduce the overall size ($0.05\lambda_g \times 0.036\lambda_g$ at 900 MHz). Each device is the combination of lattice lumped structure with a low-pass filter and a high-pass filter configuration. This structural formation of lumped elements helps to reduce the phase mismatch error in the balun devices. For all the balun devices, the measured results indicated a minimum amplitude imbalance (<0.47 dB) and low phase imbalance ($180 \pm 2.6°$). Mathematically calculated, calculated after considering parasitic effects, simulated and measured results exhibited a good correlation. The return loss is below 18 dB and insertion loss is below 0.25 dB for the entire fabricated devices. A balun device with a center frequency of 900 MHz has given the best results amongst all fabricated devices.

INDEX TERMS Integrated passive device (IPD), gallium arsenide (GaAs), MIM capacitor, spiral inductor.

I. INTRODUCTION

Balun is a vital component that works as subordinate for numerous microwave devices requiring differential signal. It isolates input signal into two output signal each with half amplitude and 180° phase shift [1], [2]. The basic purpose of balun is to transfer signal in-between two diverse transmission environments with minimal power loss [3]. In the circuit level, balun has been used with several devices such as double balanced mixers, frequency multipliers, antennas, and push-pull amplifiers [4]–[8]. Several passive balun designs such as Marchand type [9], [10], Wilkinson type [11], [12], hybrid type [13], [14], lumped-element type [15], [16], and microstrip type [17], [18] have been previously reported. Balun design concepts are broadly classified into distributed and lumped form. The distributed type balun devices are the combination of quarter wavelength coupled line resonators. These types of balun devices acquire large bandwidth and correlated phase [19]. But they occupy large area at low frequencies (<5 GHz) due to quarter-wavelength coupled lines [20], [21]. Similarly, the lumped type balun devices are constructed using multiple units of lattice resistor (R), inductor (L) and capacitor (C) structure or low pass filter (LPF) and high pass filter (HPF) lumped element structures [22]. These types of balun devices require small area as compared to distributed type but they exhibit high losses, narrow bandwidth and large phase imbalance [23]. Since, most conventional microwave passive component designs are based on transmission line concept and they occupy large area. Due to the problem of acquiring large area at low frequencies, they have become a bottleneck problem for the size reduction in microwave front-end [24]. Various works have been proposed

The associate editor coordinating the review of this manuscript and approving it for publication was Xiaoguang Leo Liu.

to reduce the structure size of microwave passive component design. Currently, lattice type balun design based on symmetrical π-structure of lumped elements in low and high pass filter configuration has become a good candidate for microwave passive device designs due to its compact layouts and small size [15], [25]. The introduction of the capacitive component along with the inductive component helps to increase the overall reactive impedance of the circuit and helps inductor to act as a transformer [26]. Moreover, the combination of LPF and HPF in the design structure can also be used to reduce the phase mismatch error [23]. Although, the minimal structure size achievable at low frequency is usually limited by the fabrication process such as minimum possible fabricated line width and the gap width [27]. Integrated passive device (IPD) fabrication is one of the best possible solutions to produce high-quality and miniaturized size passive devices [28]. Recently, Gallium Arsenide (GaAs) substrate based IPD technology has been considered as a best candidate for lumped element implementation due to its high substrate resistivity and low substrate loss [29], [30]. The high resistivity of a substrate helps to reduce coupling losses between lumped components, suppresses substrate noise, and minimizes parasitic effects such as stray capacitance and stray inductance at high frequency [31]. Low loss substrate helps to minimize eddy current loss and increase Q value of lumped elements [32]. The fabricated devices using IPD technique also shows good compatibility to integrate into the system-in-package or system-on-chip environment using multichip modules (MCMs) [28].

In this paper, we presented three highly selective, low loss and miniaturized lumped element based balun devices fabricated through IPD technology on GaAs substrate for different center frequencies.

Design analysis of individual balun device is evaluated after comparing the mathematically calculated, calculated with parasitic effects, simulated and fabricated results. The fabricated balun structures are suitable for telecom industries, where miniaturization and integration are necessary. The compact dimensions of balun devices are 1.2 mm × 1.8 mm × 0.2 mm, 1 mm × 1.5 mm × 0.2 mm and 1 mm × 1.4 mm × 0.2 mm at center frequency of 900 MHz, 1800 MHz and 2400 MHz, respectively.

II. MATHEMATICAL ANALYSIS

The proposed balun devices are based on lattice structure of lumped type *LC* elements placed in LPF and HPF configuration, where, $L_1 = L_2$ and $C_1 = C_2$. The circuit configuration of lumped element based balun device in π-network is shown in Fig. 1(a). To achieve better impedance matching and minimum phase imbalance the output ports of this configuration are formed quarter wavelength apart [33], [34]. The transmission or ABCD parameters for an ideal lossless transmission line (attenuation, $\alpha = 0$) is written as [35],

$$\begin{bmatrix} A & B \\ C & D \end{bmatrix} = \begin{bmatrix} \cos\beta l & jZ_0 \sin\beta l \\ jY_0 \sin\beta l & \cos\beta l \end{bmatrix} \quad (1)$$

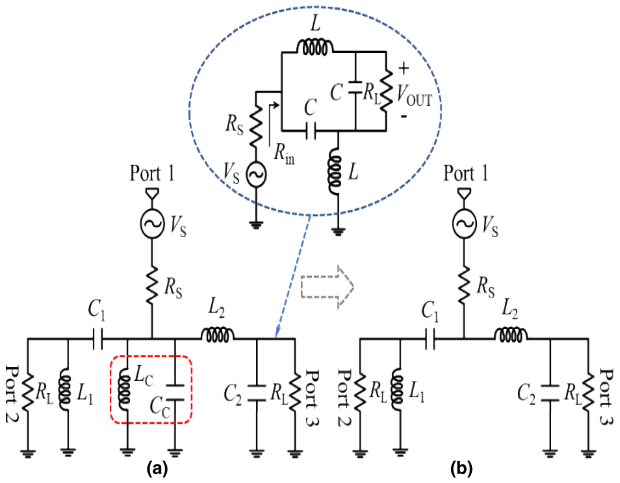

FIGURE 1. (a) Basic π-type circuit of lumped type balun device. (b) Compensated circuit of lumped type balun device.

where,

Z_0 represents characteristic impedance
β represents wave phase shift per unit length
l represents length of transmission line
Y_0 represents characteristic admittance of transmission

The output ports of balun device can be represented with quarter-wave and odd multiples of quarter-wave transmission line. The output ports of the lumped circuits are formed $\lambda/4$ and $3\lambda/4$ apart, that makes $\beta l = 90°$ and 270° [36]. After substituting the value of βl, (1) can be rewritten as:
when, $\beta l = 90°$

$$\begin{bmatrix} A & B \\ C & D \end{bmatrix} = \begin{bmatrix} 0 & jZ_0 \\ jY_0 & 0 \end{bmatrix} \quad (2)$$

and when $\beta l = 270°$

$$\begin{bmatrix} A & B \\ C & D \end{bmatrix} = \begin{bmatrix} 0 & -jZ_0 \\ -jY_0 & 0 \end{bmatrix} \quad (3)$$

For quarter-wave transformer,

$$Z_0 = \sqrt{Z_{in} Z_L} \quad (4)$$

To simplify analysis, ABCD parameter is applied to the individual arm of the presented balun circuit in Fig. 1(b).

Series inductor can be represented as,

$$\begin{bmatrix} A & B \\ C & D \end{bmatrix} = \begin{bmatrix} 1 & jX_L \\ 0 & 1 \end{bmatrix} \quad (5)$$

Similarly, shunt capacitor can be represented as,

$$\begin{bmatrix} A & B \\ C & D \end{bmatrix} = \begin{bmatrix} 1 & 0 \\ jB_C & 1 \end{bmatrix} \quad (6)$$

Moreover, series capacitor can be represented as,

$$\begin{bmatrix} A & B \\ C & D \end{bmatrix} = \begin{bmatrix} 1 & -jX_C \\ 0 & 1 \end{bmatrix} \quad (7)$$

Also, shunt inductor can be represented as,

$$\begin{bmatrix} A & B \\ C & D \end{bmatrix} = \begin{bmatrix} 1 & 0 \\ -jB_L & 1 \end{bmatrix} \quad (8)$$

LPF is the combination of series inductor and shunt capacitor in cascaded form. Therefore, the transmission parameter for LPF can be extracted from (5) and (6),

$$\begin{bmatrix} A & B \\ C & D \end{bmatrix} = \begin{bmatrix} 1 & jX_L \\ 0 & 1 \end{bmatrix} \begin{bmatrix} 1 & 0 \\ jB_C & 1 \end{bmatrix} \tag{9}$$

$$\begin{bmatrix} A & B \\ C & D \end{bmatrix} = \begin{bmatrix} 1 - B_C X_L & jX_L \\ jB_C & 1 \end{bmatrix} \tag{10}$$

where, $X_L = \omega L$ and $B_C = \omega C$

Similarly, HPF is the combination of series capacitor and shunt inductor in cascaded form. Therefore, the transmission parameter for HPF can be extracted from (7) and (8),

$$\begin{bmatrix} A & B \\ C & D \end{bmatrix} = \begin{bmatrix} 1 & -jX_C \\ 0 & 1 \end{bmatrix} \begin{bmatrix} 1 & 0 \\ -jB_L & 1 \end{bmatrix} \tag{11}$$

$$\begin{bmatrix} A & B \\ C & D \end{bmatrix} = \begin{bmatrix} 1 + jB_L X_C & -jX_C \\ -jB_L & 1 \end{bmatrix} \tag{12}$$

where, $X_C = \frac{1}{\omega C}$ and $B_L = \frac{1}{\omega L}$.

The inductance and capacitance value can be evaluated after comparing (2) with (9) and (3) with (11) respectively,

$$L = \frac{Z_0}{\omega} \tag{13}$$

$$C = \frac{1}{Z_0 \omega} \tag{14}$$

where, $\omega =$ angular frequency

The evaluated value of discrete L and C components extracted from (13) and (14) is shown in Table 1. The input impedance of 50 Ω and output impedance of 300 Ω is considered for calculation purpose. The selected center frequency for the theoretical calculation is based on GSM and broadband services (900 MHz, 1800 MHz and 2400 MHz) in mobile communication.

TABLE 1. Theoretical value of *L* and *C* in lumped type balun device.

f_0[a](MHz)	Z_{in}(Ω)	Z_L (Ω)	Z_0 (Ω)	L (nH)	C (pF)
900	50	300	122.47	21.66	1.44
1800	50	300	122.47	10.83	0.72
2400	50	300	122.47	8.12	0.54

[a]f_0 = Centre Frequency

III. DESIGN AND SIMULATION

A. PARASITIC EFFECTS

In microwave frequencies, the lumped elements such as inductor (L), capacitor (C) and resistor (R) suffer from parasitic reactance due to the existing fringing fields. These lumped components such as L and C store or release electric and magnetic fields during their high frequency operations. These released fields act as stray capacitance and inductance inside the circuit and degrade output results. This involvement of unintentionally formed components generates parasitic effect inside the circuit. In IPD devices, the effect of ground plane, substrate material losses and thickness, conductor material losses and thickness, fringing field, proximity effect play an important role for the presence of such parasitic effects. These effects induce shift in the desired resonating frequency [37], [38]. It is necessary to analyze the involvement of parasitic effects prior to fabrication of device using IPD technique. The fabricated design is the combination of two on-chip spiral inductors and two metal-insulator-metal (MIM) capacitors in LPF and HPF configuration. The size of spiral inductors is considered small to reduce parasitic losses and increase integration. The reduction in overall parasitic losses in the devices helps to minimize insertion loss and improve return loss [32]. Prior to fabricating the balun devices the value of parasitic effects in MIM capacitor and spiral inductor have been evaluated and replaced with a small circuit of lumped elements. The equivalent circuit for MIM capacitor and spiral inductor is shown in Fig. 2. Furthermore, the ideal value of L and C components discussed in Fig. 1(b) are replaced with the simulated values through NI AWR design environment to realize the actual effect of fabricated spiral inductor and MIM capacitor equivalent circuits of MIM capacitor and spiral inductor shown in Fig. 2 for further analysis. The obtained circuit is in the circuit after fabrication. The equivalent circuit of balun devices after involving the extracted form of lumped element is shown in Fig. 3. The values of the calculated model parameters after considering all the parasitic effects and a design dimension error are shown in Table 2 (a) and (b), respectively.

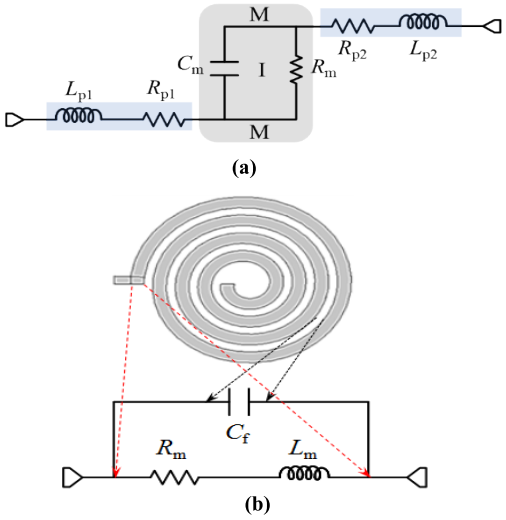

FIGURE 2. Equivalent circuit of lumped element designed by IPD process. (a) MIM capacitor. (b) Spiral inductor.

In model parameter of MIM capacitor, L_{P1} and R_{P1} represent inductance and resistance of lower plate, C_m and R_m represent capacitance and resistance due to dielectric material present in-between conductive plates and finally, L_{P2} and R_{P2} represent inductance and resistance of upper plate. Similarly, in model parameter of spiral inductor, L_m and R_m represent inductance and resistance of conductive metal. Also, C_f represents the capacitance effect exists due to the gap present in between conductive spiral lines. The effect of other parameters like co-planar waveguide with ground (CPWG) and transmission line (TML) is also considered during circuit simulation.

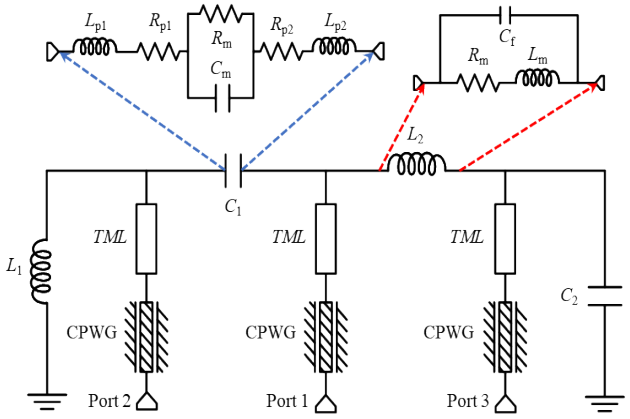

FIGURE 3. Equivalent circuit of balun devices including possible design errors.

TABLE 2. (a) Calculated model parameter value of MIM capacitor. (b) Calculated model parameter value of spiral inductor.

(a)

f_0[a] (MHz)	L_{P1}(pH)	R_{P1} (Ω)	R_m(MΩ)	C_m(pF)	L_{P2}(pH)	R_{P2} (Ω)
900	87.36	0.06	1	2.49	64.84	0.07
1800	92.80	0.12	1	1.25	67.20	0.14
2400	83.73	0.11	1	0.92	60.49	0.13

[a]f_0 = Centre Frequency

(b)

f_0[a] (MHz)	L_m (nH)	R_m (Ω)	C_f (fF)
900	12.49	1.08	19.47
1800	6.61	0.66	16.98
2400	4.18	0.46	12.01

[a]f_0 = Centre Frequency

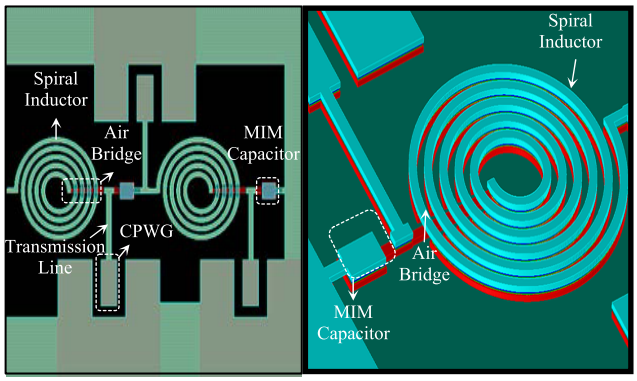

FIGURE 4. Simulated balun device. (a) Top view. (b) 3-D view.

B. SIMULATED DESIGN

The proposed balun devices consist of two spiral inductors with equal number of turns and equal inner diameter. Similarly, two MIM capacitors of similar effective area are used to convert inductor as a transformer [26]. The proposed balun devices were simulated using Advance Design System (ADS) simulation software at center frequencies of 900 MHz, 1800 MHz and 2400 MHz, respectively. The top view and perspective view of the simulated balun device is shown in Fig. 4.

TABLE 3. Dimensions of lumped devices in simulated balun device.

f_0[a] (MHz)	Balun Device		Spiral Inductor		MIM Capacitor	
	L[b] (mm)	W[c] (mm)	D[d] (μm)	T[e]	L[b] (μm)	W[c] (μm)
900	1.8	1.2	150	06	75	100
1800	1.5	1	100	05	75	50
2400	1.4	1	100	04	55	50

[a]f_0 = Center Frequency, [b]L = Length, [c]W = Width, [d]D = Diameter of Spiral, [e]T = Number of Spiral Turns

The selection of central frequency is based on the dimensions of spiral inductor and MIM capacitor. The inductance value of design is based on the diameter and number of turns of spiral inductor, whereas the capacitance value is based on the effective area of MIM capacitor [38]. The dimensions of simulated and fabricated balun devices along with spiral inductor and MIM capacitor dimensions at different center frequencies is shown in Table 3.

IV. FABRICATION

The IPD fabrication method and steps play a vital role to fabricate an error-free balun device. The following process of IPD fabrication used to fabricate all balun devices. Firstly, a 6 inch GaAs wafer is procured and then cleaned with acetone, Iso-Propyl Alcohol and DI water, respectively. Later on, silicon nitride (Si_3N_4) was deposited on the wafer using plasma enhanced chemical vapor deposition process. Si_3N_4 was used for wafer passivation and to increase the adhesion between wafer and first seed metal layer. Then, photoresist was patterned to form a desired structure on wafer. After that, first seed metal of Ti/Au was deposited via sputtering process and then Cu/Au was deposited using electroplating process. The thickness of total metal was considered as 5 μm to reduce skin effect loss and make process cost effective. In the next step, dry etching was used to remove undesired seed metal layer and then used acetone to remove unwanted photoresist. Then again Si_3N_4 layer was deposited to prevent shortage between top metal and bottom metal and form an insulator for MIM capacitor.

Another important and complex task was to form air-bridge post. Firstly, photoresist coating was done and then air bridge seed metal of Ti/Au was formed using sputtering followed by the deposition of Cu/Au through electroplating process. Again acetone was used to remove undesired photoresist. Afterwards, reactive-ion-etching was used to remove undesired seed metal part. In last, Si_3N_4 was coated to form final passivation layer. The IPD based balun structure, layer information and cross-sectional focused ion beam (FIB) image of device is shown in Fig. 5.

V. RESULTS AND DISCUSSIONS

To validate the proposed design of baluns, the mathematically calculated, calculated with parasitic effects, simulated and measured S-parameter and phase response of designed balun devices at 900 MHz, 1800 MHz and 2400 MHz are compared. It can be observed from Fig. 6(a) that there is a good correlation between mathematically calculated (MC), calculated after considering parasitic effects (PE), simulated (SM)

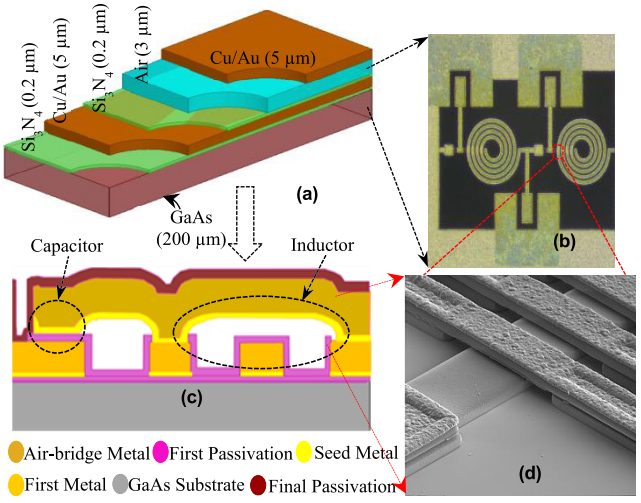

FIGURE 5. (a) Layer information of a fabricated a balun device. (b) A fabricated balun device. (c) Cross-sectional view to show formation of lumped elements after IPD fabrication. (d) FIB image of the air-bridge structure.

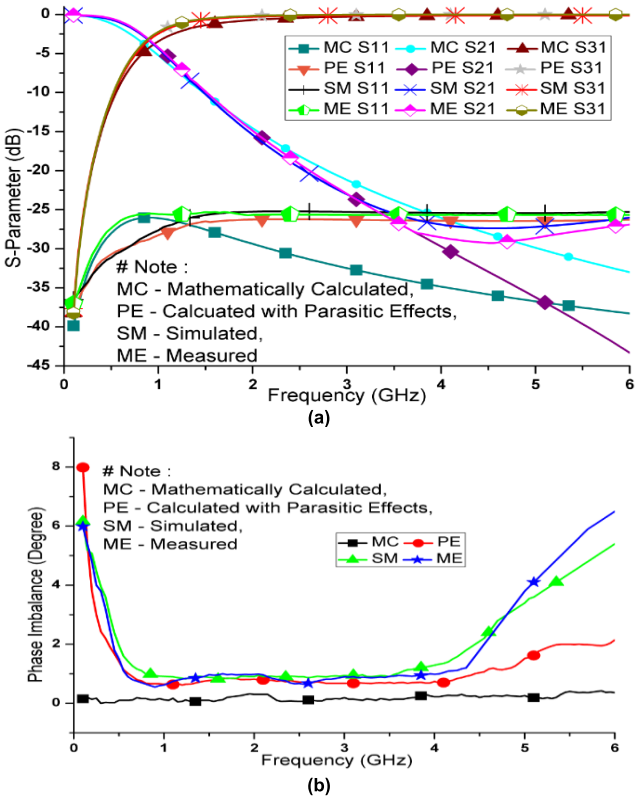

FIGURE 6. Comparison of calculated, simulated, and measured results at 900 MHz. (a) Magnitude response. (b) Phase imbalance.

and measured (ME) S-parameters. The evaluated S-parameter at 900 MHz shows the amplitude imbalance of 0.02 dB, 0.012 dB, 0.008 dB and 0.002 dB in MC, PE, SM and ME, respectively. Similarly, the phase imbalance of 180 ± 2.6° in-between 0.5 - 4 GHz for MC, PE, SM and ME results is shown in Fig. 6(b). The measured results show return loss higher than 25 dB and insertion loss lower than 0.2 dB at 900 MHz.

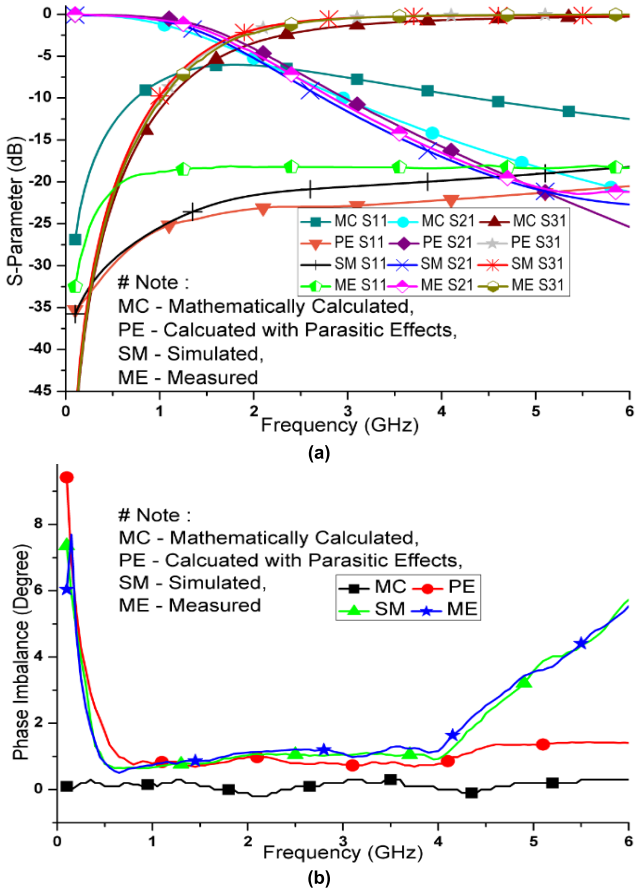

FIGURE 7. Comparison of calculated, simulated, and measured results at 1800 MHz. (a) Magnitude response. (b) Phase imbalance.

Moreover, the S-parameters, which were evaluated at the central frequency of 1800 MHz and are shown in Fig. 7(a), indicated a good agreement among MC, PE, SM and ME S-parameters with amplitude imbalance of 0.002 dB, 0.29 dB, 0.25 dB and 0.35 dB, respectively. In addition, a good correlation among phase response of balun device operating at 1800 MHz was obtained and is shown in Fig. 7(b). The measured phase imbalance is 180 ± 2.5° for the frequency range of 0.5 - 4 GHz. The measured return loss is higher than 18 dB and insertion loss is lower than 0.25 dB at 1800 MHz.

Furthermore, the S-parameters and phase imbalances of a balun (2400 MHz), which are shown in Fig. 8 (a) and (b), indicated a good match among MC, PE, SM and ME with amplitude imbalance of 0.009 dB, 0.35 dB, 0.1 dB and 0.47 dB and phase imbalance of 180 ± 3° for a frequency range of 0.5 - 5 GHz. The measured return loss and insertion loss was higher than 21 dB and lower than 0.24 dB, respectively.

Table 4, which compares the various performance parameters of the proposed balun devices with several previously reported baluns, indicates that our developed balun devices have exhibited the smallest amplitude and phase imbalance, which can be attributed to the symmetrically configured LPF and HPF-based layout of the illustrated balun devices. In addition, the proposed baluns have exhibited more

TABLE 4. Performance comparison of the proposed baluns with several reported baluns.

Ref.	f_0^a (MHz)	Fabrication	Return Loss (dB)	Insertion Loss (dB)	Amplitude Imbalance (dB)	Phase Imbalance (°)	Effective Area (mm^2)
10	5500	LTCC	Not Available	1.76	0.6	5	0.089 $\lambda_g \times$ 0.076 λ_g
14	2200	LTCC	>10	2.26	0.4	3.2	0.067 $\lambda_g \times$ 0.042 λ_g
18	2880	PCB	17	5.1	0.49	6.5	0.1 $\lambda_g \times$ 0.1 λ_g
19	1000	PCB	19	0.8	0.35	5	0.586 $\lambda_g \times$ 0.317 λ_g
20	6500-28500	IPD	Not Available	3.69	1	1.65	Not Available
21	4450	IPD	57.9	0.75	0.49	6.2	Not Available
	900		**25**	**0.2**	**0.002**	**2.6**	**0.05 $\lambda_g \times$ 0.036 λ_g**
This work	**1800**	**IPD**	**18**	**0.25**	**0.35**	**2.5**	**0.032 $\lambda_g \times$ 0.021 λ_g**
	2400		**21**	**0.24**	**0.45**	**2.6**	**0.04 $\lambda_g \times$ 0.028 λ_g**

f_0^a = Center Frequency

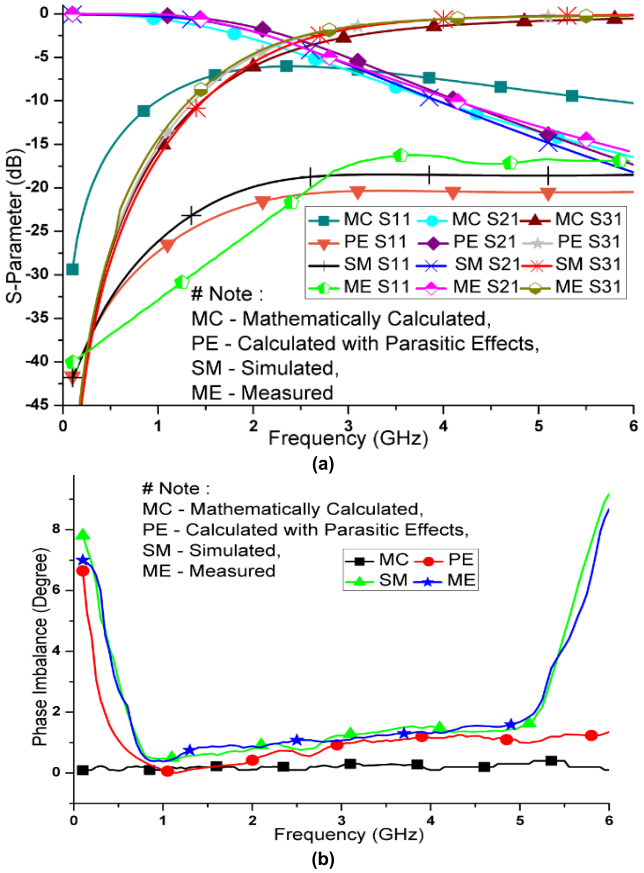

FIGURE 8. Comparison of calculated, simulated, and measured results at 2400 MHz. (a) Magnitude response. (b) Phase imbalance.

compact size and better selectivity. Moreover, the reduced parasitic loss of the device due to the high-resistivity GaAs substrate and compact on-chip spiral inductor resulted in excellent insertion and return losses.

VI. CONCLUSION

In this paper, highly selective, low-loss and miniaturized balun devices with central frequencies of 900 MHz, 1800 MHz (GSM band) and 2400 MHz (Wi-Fi band) have been proposed, simulated and fabricated using GaAs-IPD technology. The lumped elements-based symmetric LPF and HPF configuration fabricated on a high-resistivity GaAs substrate helps to achieve low insertion loss, minimize phase and amplitude imbalance and miniaturize balun devices. The calculated and simulated results are compared with measured results to indicate fabrication errors. To minimize the fabrication errors in design, all parasitic effects were considered during calculation and simulation. The fabricated balun devices indicated amplitude imbalance of 0.002 dB, 0.35 dB and 0.47 dB and phase imbalance of 2.6°, 2.5° and 2.6° at central frequency 900 MHz, 1800 MHz and 2400 MHz, respectively.

ACKNOWLEDGEMENT

Alok Kumar would like to thank Cong Wang and Tian Qian for technical support and fabrication, Fan Yi Meng, Qun Wu and Yongle Wu for guidance. Special thank has given to Kishor Kumar Adhikari for co-writing this manuscript.

REFERENCES

[1] J.-M. Yan, H.-Y. Zhou, and L.-Z. Cao, "A novel filtering balun and improvement of its isolation performance," *IEEE Microw. Wireless Compon. Lett.*, vol. 27, no. 12, pp. 1056–1058, Dec. 2017.

[2] Y. Wang and J.-C. Lee, "A miniaturized Marchand balun model with short-end and capacitive feeding," *IEEE Access*, vol. 6, pp. 26653–26659, 2018.

[3] R. C. Frye, G. Badakere, Y. Lin, and M. P. Chelvam, "A monolithic, compact balun/matching network for SiP applications," in *Proc. IEEE Conf. Elect. Perform. Electron. Packag.*, Oct. 2004, pp. 37–40.

[4] W. S. Yeoh, K. L. Wong, and W. S. T. Rowe, "Wideband miniaturized half bowtie printed dipole antenna with integrated balun for wireless applications," *IEEE Trans. Antennas Propag.*, vol. 59, no. 1, pp. 339–342, Jan. 2011.

[5] K. W. Hamed, A. P. Freundorfer, and Y. M. M. Antar, "A monolithic double-balanced direct conversion mixer with an integrated wideband passive balun," *IEEE J. Solid-State Circuits*, vol. 40, no. 3, pp. 622–629, Mar. 2005.

[6] H. T. Jeong, M. H. Yeon, S. W. Kim, and I. S. Chang, "Design of the Doherty amplifier with push-pull structure using balun transformer," in *IEEE MTT-S Int. Microw. Symp. Dig.*, Jun. 2004, pp. 851–854.

[7] S. Gerlich and P. Weger, "Highly efficient packaged 11–13 GHz power amplifier in SiGe-technology with 37.3% of PAE," *IEEE Microw. Wireless Compon. Lett.*, vol. 23, no. 10, pp. 539–541, Oct. 2013.

[8] I. Kallfass, A. Tessmann, H. Massler, S. Wagner, and A. Leuther, "A 480 GHz active frequency multiplier-by-four SMMIC," in *IEEE MTT-S Int. Microw. Symp. Dig.*, Jun. 2012, pp. 1–3.

[9] C.-H. Tseng and Y.-C. Hsiao, "A new broadband Marchand balun using slot-coupled microstrip lines," *IEEE Microw. Wireless Compon. Lett.*, vol. 20, no. 3, pp. 157–159, Mar. 2010.

[10] J.-X. Xu, X. Y. Zhang, and X.-L. Zhao, "Compact LTCC balun with bandpass response based on Marchand balun," *IEEE Microw. Wireless Compon. Lett.*, vol. 26, no. 7, pp. 493–495, Jul. 2016.

[11] J.-S. Lim, H.-S. Yang, Y.-T. Lee, S. Kim, K.-S. Seo, and S. Nam, "E-band Wilkinson balun using CPW MMIC technology," *Electron. Lett.*, vol. 40, no. 14, pp. 879–881, Jul. 2004.

[12] W.-K. Lee and H.-Y. Hwang, "Size and harmonic reduced Wilkinson balun using parallel coupled line with open stub," *J. Electromagn. Eng. Sci.*, vol. 14, no. 4, pp. 387–392, Dec. 2014.
[13] E. Y. Jung and H. Y. Hwang, "A balun-BPF using a dual mode ring resonator," *IEEE Microw. Wireless Compon. Lett.*, vol. 17, no. 9, pp. 652–654, Sep. 2007.
[14] T. Yang, M. Tamura, and T. Itoh, "Compact and high-performance low-temperature co-fired ceramic balun filter using the hybrid resonator and symmetric four-port network," *IEEE Trans. Antennas Propag.*, vol. 6, no. 2, pp. 121–126, Jan. 2012.
[15] D. Kuylenstierna and P. Linner, "Design of broadband lumped element baluns," in *IEEE MTT-S Int. Microw. Symp. Dig.*, Jun. 2004, pp. 899–902.
[16] V. Gonzalez-Posadas, C. Martin-Pascual, J. L. Jimenez-Martin, and D. Segovia-Vargas, "Lumped-element balun for UHF UWB printed balanced antennas," *IEEE Trans. Antennas Propag.*, vol. 56, no. 7, pp. 2102–2107, Jul. 2008.
[17] H.-X. Xu, G.-M. Wang, X. Chen, and T.-P. Li, "Broadband balun using fully artificial fractal-shaped composite right/left handed transmission line," *IEEE Microw. Wireless Compon. Lett.*, vol. 22, no. 1, pp. 16–18, Jan. 2012.
[18] Y. Geng, W. Wang, X. Chen, L. Han, L. Li, and W. Zhang, "The study and design of a miniaturized microstrip balun with a wider bandwidth," *IEEE Antennas Wireless Propag. Lett.*, vol. 15, pp. 1727–1730, 2016.
[19] C. Cai, J. Wang, L. Zhu, and W. Wu, "A new approach to design microstrip wideband balun bandpass filter," *IEEE Microw. Wireless Compon. Lett.*, vol. 26, no. 2, pp. 116–118, Feb. 2016.
[20] H. J. Qian and X. Luo, "Compact 6.5-28.5 GHz on-chip balun with enhanced inband balance responses," *IEEE Microw. Wireless Compon. Lett.*, vol. 26, no. 12, pp. 993–995, Dec. 2016.
[21] H.-Y. Chung, H.-K. Chiou, Y.-C. Hsu, T.-Y. Yang, and C.-L. Chang, "Design of step-down broadband and low-loss Ruthroff-type baluns using IPD technology," *IEEE Trans. Compon., Packag. Manuf. Technol.*, vol. 4, no. 6, pp. 967–974, Jun. 2014.
[22] W. Bakalski, W. Simburger, H. Knapp, H.-D. Wohlmuth, and A. L. Scholtz, "Lumped and distributed lattice-type LC-baluns," in *IEEE MTT-S Int. Microw. Symp. Dig.*, Jun. 2002, pp. 209–212.
[23] H.-K. Chiou, H.-H. Lin, and C.-Y. Chang, "Lumped-element compensated high/low-pass balun design for MMIC double-balanced mixer," *IEEE Microw. Guided Wave Lett.*, vol. 7, no. 8, pp. 248–250, Aug. 1997.
[24] E. Pettenpaul, H. Kapusta, A. Weisgerber, H. Mampe, J. Luginsland, and I. Wolff, "CAD models of lumped elements on GaAs up to 18 GHz," *IEEE Trans. Microw. Theory Techn.*, vol. MTT-36, no. 2, pp. 294–304, Feb. 1988.
[25] D. Kuylenstierna and P. Linnér, "Design of broad-band lumped-element baluns with inherent impedance transformation," *IEEE Trans. Microw. Theory Techn.*, vol. 52, no. 12, pp. 2739–2745, Dec. 2004.
[26] C.-F. Chang and Y.-S. Lin, "On-chip transformer-coupled balun bandpass filter for 5-GHz applications," in *IEEE MTT-S Int. Microw. Symp. Dig.*, May 2015, pp. 1–4.
[27] K.-Y. Chen, B.-X. Fang, and H.-H. Yeh, "IPD broadband balun design for GSM applications," in *Proc. IEEE Elect. Design Adv. Package Syst. Symp.*, Dec. 2010, pp. 1–4.
[28] T.-C. Tang and K.-H. Lin, "MIMO antenna design in thin-film integrated passive device," *IEEE Trans. Compon., Packag., Manuf. Technol.*, vol. 4, no. 4, pp. 648–655, Apr. 2014.
[29] C. Wang, W. S. Lee, F. Zhang, and N. Y. Kim, "A novel method for the fabrication of integrated passive devices on SI-GaAs substrate," *Int. J. Adv. Manuf. Technol.*, vol. 52, nos. 9–12, pp. 1011–1018, Feb. 2011.
[30] C. Wang *et al.*, "Room temperature fabrication of MIMCAPs via aerosol deposition," *IEEE Electron Device Lett.*, vol. 37, no. 2, pp. 220–223, Feb. 2016.
[31] H. Jeon and K. W. Kobayashi, "Comparison of 5-GHz quadrature couplers using GaAs and silicon-based IPD technologies," *IEEE Microw. Wireless Compon. Lett.*, vol. 28, no. 9, pp. 756–758, Sep. 2018.
[32] Z. Zhang and X. Liao, "Micromachined passive bandpass filters based on GaAs monolithic-microwave-integrated-circuit technology," *IEEE Trans. Electron Devices*, vol. 60, no. 1, pp. 221–228, Jan. 2013.
[33] D.-W. Lew, J.-S. Park, D. Ahn, N.-K. Kang, C. S. Yoo, and J. B. Lim, "A design of the ceramic chip balun using the multilayer configuration," *IEEE Trans. Microw. Theory Techn.*, vol. 49, no. 1, pp. 220–224, Jan. 2001.
[34] C.-S. Yoo *et al.*, "RF front-end passive circuit implementation including antenna for ZigBee applications," *IEEE Trans. Microw. Theory Techn.*, vol. 55, no. 5, pp. 906–915, May 2007.
[35] D. M. Pozar, *Microwave Engineering*, 2nd ed. New York, NY, USA: Wiley, 1997.
[36] S. J. Parisi, "180 degrees lumped element hybrid," in *IEEE MTT-S Int. Microw. Symp. Dig.*, Jun. 1989, pp. 1243–1246.
[37] J. S. Joshi, J. R. Cockrill, and J. A. Turner, "Monolithic microwave gallium arsenide FET oscillators," *IEEE Trans. Electron Devices*, vol. ED-28, no. 2, pp. 158–162, Feb. 1981.
[38] I. J. Bahl, *Lumped Elements for RF and Microwave Circuits*. London, U.K.: Artech House, 2003.

ALOK KUMAR was born in New Delhi, India, in 1991. He received the bachelor's and master's degrees in electronics and communication engineering from Punjab Technical University, Jalandhar, India, in 2012 and 2016, respectively. He is currently pursuing the Ph.D. degree with the Department of Electronics and Information Engineering, Harbin Institute of Technology, China. His research interests include microwave antenna designing, sensors, microwave passive components, substrate integrated waveguide, and optical communication links.

FAN-YI MENG (S'07–M'09–SM'15) received the B.S., M.S., and Ph.D. degrees in electromagnetics from the Harbin Institute of Technology, Harbin, China, in 2002, 2004, and 2007, respectively, where he has been with the Department of Microwave Engineering, since 2007, and is currently a Professor. He has co-authored four books, 40 international refereed journal papers, over 20 regional refereed journal papers, and 20 international conference papers. His current research interests include antennas, electromagnetic and optical metamaterials, plasmonics, and electromagnetic compatibility.

Dr. Meng was a recipient of several awards, including the 2013 Top Young Innovative Talents of the Harbin Institute of Technology, the 2013 CST University Publication Award, the 2010 Award of Science and Technology from the Heilongjiang Province Government of China, the 2010 Microsoft Cup IEEE China Student Paper Contest Award, two Best Paper Awards from the National Conference on Microwave and Millimeter Wave in China (in 2009 and 2007), the 2008 University Excellent Teacher Award of the National University of Singapore, the 2007 Excellent Graduate Award of Heilongjiang Province of China, and the Outstanding Doctor Degree Dissertation Award of the Harbin Institute of Technology.

CONG WANG (S'08–M'11–SM'16) was born in Qingdao, Shandong, China, in 1982. He received the B.S. degree in automation engineering from Qingdao Technological University, China, in 2005, and the M.S. and Ph.D. degrees in electronic engineering from Kwangwoon University, Seoul, South Korea, in 2008 and 2011, respectively. In 2007, he was a Research Engineer with the Research and Development Department, Mission Technology Co., Ltd, Gyeonggi, South Korea, where he was involved in the development of microwave components and devices using hybrid and LTCC technology. He joined the Research and Development Department, NanoENS Co., Ltd, in 2007. In 2011, he joined the Department of Electronic Engineering, Kwangwoon University, as an Assistant Professor. He joined the Harbin Institute of Technology in 2016, where he is currently a Professor. He was involved in passive device modeling, passive device design, and fabrication process development and optimization. He has co-authored two books and published more than 220 papers in domestic and international journals and conferences. He has over 40 patents registered in South Korea. His major interests include RFIC/MMIC design and semiconductor fabrication development, such as GaAs integrated passive devices, GaAs PIN diodes, GaAs Schottky barrier diodes, and AlGaN/GaN high electron mobility transistors; silicon-based LED module fabrication and packaging; and various types of smart IoT sensors and their applications, which are emerging advanced semiconductor fabrication technologies.

KISHOR KUMAR ADHIKARI received the Ph.D. degree in electronic engineering from Kwangwoon University, Seoul, South Korea, in 2016. He is currently a Research Associate with the Department of Microwave Engineering, School of Astronautics, Harbin Institute of Technology, Heilongjiang, China. He has published 12 peer-reviewed journal papers and 16 international conference papers. He holds two research patents. His research interests include microwave resonant biosensors, micro-fabrication via photolithography, nanomaterial synthesis and their integration with microfabricated biosensors, and conformal biosensors. He was a recipient of the Best Student Paper (runner-up) of the IEEE IMWS-Bio 2014 Conference held in London, U.K. He has served as a reviewer for several journals.

TIAN QIANG (M'14) was born in Baiyin, Gansu, China, in 1991. He received the B.S. degree in communication engineering from the Qingdao University of Science and Technology, China, in 2013, and the Ph.D. degree in electronic engineering from Kwangwoon University, Seoul, South Korea, in 2017. He is currently a Research Associate with the Department of Microwave Engineering, School of Electronics and Information Engineering, Harbin Institute of Technology, Heilongjiang, China. His research interests include microwave quantitative biosensors, micro–nano fabrication, and nanomaterial synthesis and their integration with microfabricated biosensors for non-contact and wireless sensing application.

QUN WU (M'93–SM'05) received the B.Sc. degree in radio engineering, the M.Eng. degree in electromagnetic fields and microwaves, and the Ph.D. degree in communication and information systems from the Harbin Institute of Technology, Harbin, China, in 1977, 1988, and 1999, respectively, where he has been with the School of Electronics and Information Engineering, since 1990, and is currently a Professor, the Head of the Department of Microwave Engineering, and also the Director of the Center for Microwaves and EMC. He was a Visiting Professor with Seoul National University, Seoul, South Korea, from 1998 to 1999, and the Pohang University of Science and Technology, from 1999 to 2000. He was a Visiting Professor with the National University of Singapore, from 2003 to 2010. He published several books and over 100 international and regional refereed journal papers. His recent research interests mainly include electromagnetic compatibility, metamaterials, and antennas. He is a member of the Microwave Society of the Chinese Institute of Electronics. He was a recipient of the Science and Technology Award from the Heilongjiang Provincial Government, in 2010. He is a Vice Chair of the IEEE Harbin Section and the Chair of the IEEE Harbin EMC/AP/MTT Joint Society Chapter. He was the Chair or a member of the TPC of international conferences for many times. He is a Technical Reviewer for several international journals. He is also invited to give a keynote report or invited papers in some international conferences for many times.

YONGLE WU (M'12–SM'15) received the B.Eng. degree in communication engineering and the Ph.D. degree in electronic engineering from the Beijing University of Posts and Telecommunications (BUPT), Beijing, China, in 2006 and 2011, respectively.

In 2010, he was a Research Assistant with the City University of Hong Kong, Hong Kong. In 2011, he joined BUPT, where he is currently a Full Professor with the School of Electronic Engineering. His research interests include microwave components, circuits, antennas, and wireless systems design.